Spill Trajectory Modelling Based on HF Radar Currents in the North Sea: Validation with Drifter Buoys

M. Cárdenas, A.J. Abascal, S. Castanedo, H. Chiri
Environmental Hydraulics Institute "IH Cantabria", Universidad de Cantabria
Santander, Spain
cardenasm@unican.es

M.I. Ferrer, J. Sanchez
Qualitas Remos
Madrid, Spain

R. Medina
Environmental Hydraulics Institute "IH Cantabria", Universidad de Cantabria
Santander, Spain

W.R. Turrell, S. Hughes, A. Gallego, B. Berx
Marine Scotland Science, Marine Laboratory
Aberdeen, Scotland, United Kingdom

Abstract

This work presents the calibration and validation of an oil spill forecasting and backtracking system based on HF radar currents by means of drifter buoys. The system, implemented in the Shetland-Orkney area in northern Scotland (UK), is based on the oil spill transport and fate model TESEO. The model is forced with: (1) ocean currents provided by a Long Range SeaSonde HF radar system implemented in the framework of the Brahan Project and (2) wind forecast from the Global Forecast System model (NOAA). The oil spill transport model has been calibrated and validated with 18 drifter buoys deployed in the study area as a part of the project. The model parameters (C_C: current coefficient and C_D: wind drag coefficient) were obtained by means of the Shuffled Complex Evolution method. The optimal values of the parameters were found to be C_C = 1.14 and C_D = 0.00015. The high C_C value obtained (close to 1) indicates a good agreement between the drifter-derived current field and the radar HF current measurements and represents an improvement with respect to similar studies performed using numerical currents data. The small value obtained for C_D could be related to the low-profile drifter design, aimed at minimising wind effect. The validation process was carried out through a comparison between the actual drifter paths and the numerical trajectories. After 48 hours of simulation the root mean square error was found to be 9.16 km for a mean trajectory length of 132.2 km. These results show a good agreement between actual and simulated trajectories and demonstrate the capabilities of the system for oil spill trajectory modelling.

1 Introduction

In the last decades, the United Kingdom coast has been affected by some of the most severe oil spill accidents in history: *Torrey Canyon*, 1967; *Braer*, 1993; *Sea Empres*s, 1996 (ITOPF, 2014). The most recent serious incident occurred when an important leak was detected in a flow line leading to the *Gannet Alpha* oil platform in 2011. The experience acquired in the past in crisis management demonstrated the importance of operational forecasting systems in the oil spill response (Montero et al., 2003; Castanedo et al., 2006;

Cárdenas, M., A.J. Abascal, S. Castanedo, H. Chiri, M.I. Ferrer, J. Sanchez, R. Medina, W.R. Turrell, S. Hughes, A. Gallego, and B. Berx, Spill Trajectory Modelling Based on HF Radar Currents in the North Sea: Validation with Drifter Buoys, Proceedings of the Thirty-Eighth AMOP Technical Seminar, Environment Canada, Ottawa, ON, pp. 123-142, 2015.

González et al., 2006). The accuracy of the simulations provided by an oil spill system highly depends on the accuracy of the met-ocean forcing data used to force the oil spill numerical model, usually provided by hydrodynamic and atmospheric models. These models have their own errors which may affect the accuracy of the oil spill forecasts (Edwards et al., 2006; Price et al., 2006). Regarding ocean circulation modeling, this uncertainty becomes more important in coastal areas, where the complex pattern that characterizes the currents complicates the forecasting of the current fields. In order to address this problem, high-frequency (HF) coastal radar observation systems have become an alternative to provide accurate current surface maps in real time in near-coastal environments. HF radar surface currents have been validated by several authors (Chapman et al., 1997; Chapman and Graber, 1997; Kohut et al., 2006). These works show that the remote sensing of surface currents in coastal areas using HF radar systems is an accurate technology, suitable for oceanographic practical applications such as for validation of ocean circulation models in coastal zones or backtracking oil spills looking for illegal discharges.

To study the benefits that an HF radar system could bring to the UK oceanographic community, a pioneer project for the UK was developed in northern Scotland, under the leadership of Marine Scotland Science (MSS) and as a joint effort of several institutions and companies: BP Exploration Operating Company Limited, the UK-IMON, the UK Department of Energy and Climate Change, the Met Office, Nexen Petroleum UK Ltd, the International Centre for Island Technology, QUALITAS Remos and CODAR Ocean Sensors. The main goal of this project, called the Brahan Project (http://www.thebrahanproject.com/), was to provide a fully operational Long Range SeaSonde HF radar system in the Shetland-Orkney area (Figure 1), able to measure the speed and direction of ocean currents in near real time and on an hourly basis, in a patch of the UK North Sea extending 180 km offshore around the Shetland and Orkney Islands. Moreover, in order to validate the HF radar current data two drift experiments were carried out in the framework of this project.

Within the framework of the project “NEw MetOcean Tools for the Oil and Gas Industry” (http://www.nemot4ogi.com), an oil spill forecasting and backtracking system was applied to the Shetland-Orkney area to show the capabilities of HF radar systems for oil spill preparedness and response. This system was working operationally during the period June 2014 - August 2014, before decommissioning of the Brahan HF radar system in September 2014. The core of the system was the TESEO oil spill numerical model (Abascal et al., 2007), which was forced with ocean currents provided by the Brahan Long Range SeaSonde HF radar system and wind forecast from the Global Forecast System model (NOAA) (Environmental Modeling Center, 2003). The main goal of the system was to provide short term oil spill trajectory forecasting and backtracking in the study area.

This work presents the calibration and validation of the HF-radar based oil spill forecast and backtracking system with drifting buoys. The oil spill transport model was calibrated by means of the global optimization method SCE-UA (Duan et al., 1992). The validation of the model results was carried out by comparison between actual drifter paths and simulated trajectories.

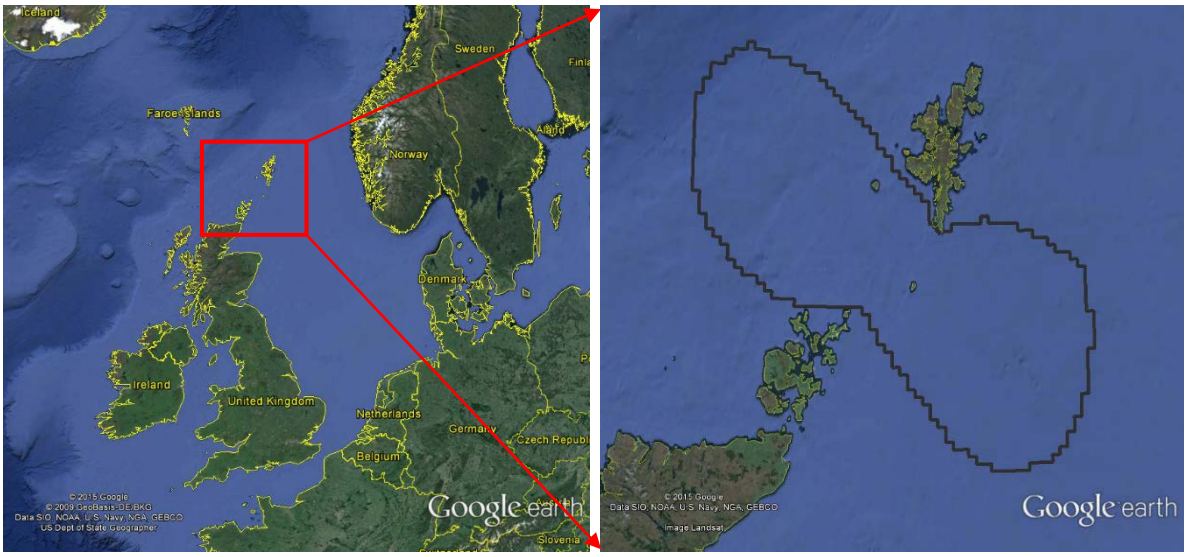

Figure 1 Study area and HF radar system domain (grey line in right panel).

2 Material and Methods

The oil spill forecasting and backtracking system based on HF radar currents was implemented in the Shetland-Orkney area (Figure 1). The system was calibrated and validated with drifter trajectories from two different drift exercises carried out in the study area. The calibration of the transport model was performed using the data collected during the first exercise and the validation with the data collected during the second one.

A description of the data and the methodology used in this study is provided in this section.

2.1 Drifter

Drifter trajectory data were collected during two drift exercises carried out by MSS as part of the Brahan Project, one in October 2013 (achieved with two different deployments, one early on and the other mid-month) and a second one in December 2013. A total of 18 drifters were deployed, ten during the first and eight during the second exercise.

The design of the drifters used to collect trajectory information was based on the work of Davis (1985). The drifters were designed to be advected by surface currents with minimal influence of wind and surface waves (Figure 2). Initial analysis of the Brahan drifter data by MSS (Berx et al., 2014) indicates that drifters show slippage through the water column, with an average of -6% (-2 cm/s slippage at a mean drift rate of 34 cm/s) in the along-drift direction, and 6% (2 cm/s slippage at a mean drift rate of 34 cm/s) in the across-drift direction.

Drifters transmitted their positions via satellite in real time with an hourly time step. Until reaching the coast or stopping transmission, they generally tracked long trajectories through the West Shetland Shelf, although in some cases just a relative small portion of the trajectories were within our study area, as shown in Figure 3.

Moreover, several gaps exist in their trajectory records due to transmission breakdowns during the drift. For these reasons, pre-processing of the drifter trajectory data was required. Taking into account the typical forecast horizon in an emergency oil spill response, 48-hour sections that remained wholly inside the HF radar domain were selected to be used as independent tracks in the study (see Table 1).

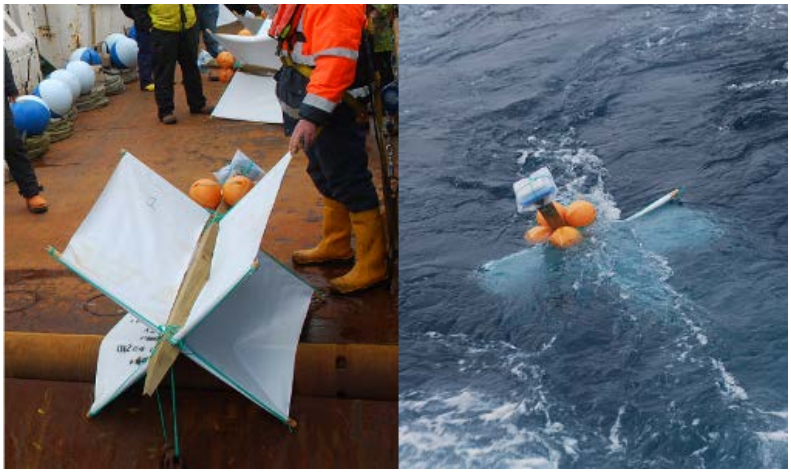

Figure 2 Photographs of drifters used in the trajectory data collection (source: Marine Scotland Science).

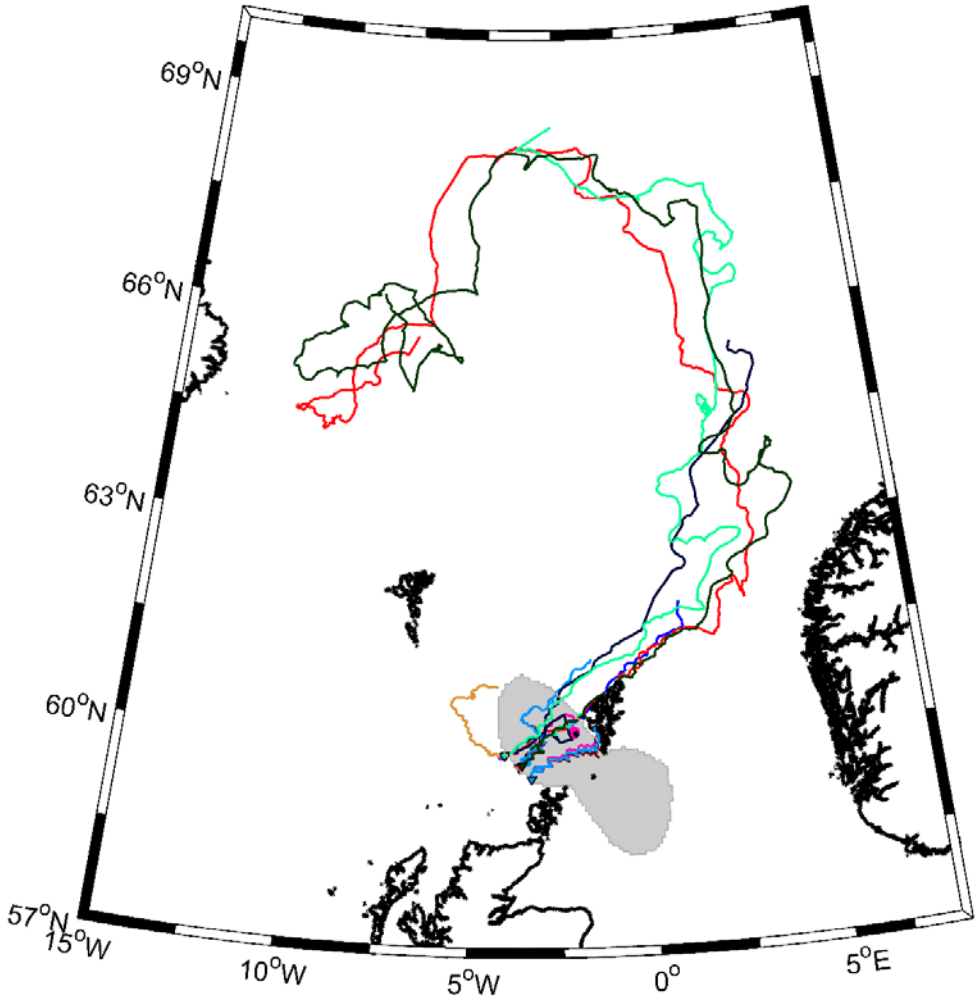

Figure 3 Trajectory data collected during the Brahan Project. The gray filled sector shows the HF radar system coverage area.

Cárdenas, M., A.J. Abascal, S. Castanedo, H. Chiri, M.I. Ferrer, J. Sanchez, R. Medina, W.R. Turrell, S. Hughes, A. Gallego, and B. Berx, Spill Trajectory Modelling Based on HF Radar Currents in the North Sea: Validation with Drifter Buoys, Proceedings of the Thirty-Eighth AMOP Technical Seminar, Environment Canada, Ottawa, ON, pp. 123-142, 2015.

Table 1 48-h sections extracted from the original trajectories.

Exercise	Section ID	Initial time	Initial position (ºE, ºN)	Final time	Last position (ºE, ºN)
1	1	2013/10/03 22:00	-3.9855, 59.8593	2013/10/05 22:00	-3.5988, 59.9360
	2	2013/10/05 22:00	-3.5988, 59.9360	2013/10/07 22:00	-2.7231, 60.3255
	3	2013/10/12 23:00	-3.6629, 59.6659	2013/10/14 23:00	-3.3935, 59.7598
	4	2013/10/12 23:00	-3.6643, 59.6660	2013/10/14 23:00	-3.3782, 59.7629
	5	2013/10/14 23:00	-3.3935, 59.7598	2013/10/16 23:00	-3.2948, 59.8758
	6	2013/10/14 23:00	-3.3782, 59.7629	2013/10/16 23:00	-3.3344, 59.8405
	7	2013/10/16 23:00	-3.2948, 59.8758	2013/10/18 23:00	-2.9552, 60.0172
	8	2013/10/16 23:00	-3.3344, 59.8405	2013/10/18 23:00	-2.9296, 60.0215
	9	2013/10/18 23:00	-2.9296, 60.0215	2013/10/20 23:00	-3.5473, 60.3441
	10	2013/10/20 23:00	-3.5473, 60.3441	2013/10/22 23:00	-3.4114, 60.4448
	11	2013/10/22 23:00	-3.4114, 60.4448	2013/10/24 23:00	-2.9071, 60.4979
	12	2013/10/24 23:00	-2.9071, 60.4979	2013/10/26 23:00	-2.7316, 60.6423
2	1	2013/12/11 3:00	-3.6435, 59.6798	2013/12/13 3:00	-3.1467, 59.9495
	2	2013/12/11 3:00	-3.6448, 59.6792	2013/12/13 3:00	-3.1487, 59.9473
	3	2013/12/13 3:00	-3.1467, 59.9495	2013/12/15 3:00	-2.0302, 60.3309
	4	2013/12/13 3:00	-3.1482, 60.2144	2013/12/15 2:00	-2.4896, 60.6181
	5	2013/12/13 3:00	-3.2541, 59.6384	2013/12/15 3:00	-2.5167, 59.7740
	6	2013/12/13 3:00	-3.2619, 59.6321	2013/12/15 3:00	-2.5140, 59.7908
	7	2013/12/11 4:00	-3.3027, 59.5101	2013/12/13 4:00	-3.2710, 59.6398
	8	2013/12/11 4:00	-3.9239, 59.8774	2013/12/13 4:00	-2.9485, 60.2916
	9	2013/12/11 4:00	-3.9363, 59.8716	2013/12/13 3:00	-3.1482, 60.2144
	10	2013/12/11 4:00	-3.3032, 59.5096	2013/12/13 4:00	-3.2586, 59.6460
	11	2013/12/11 4:00	-3.3033, 59.5102	2013/12/13 4:00	-3.2687, 59.6391
	12	2013/12/12 7:00	-3.1412, 59.8960	2013/12/14 7:00	-2.5751, 60.2294
	13	2013/12/15 4:00	-2.5055, 59.7808	2013/12/17 4:00	-1.6606, 59.8649
	14	2013/12/15 4:00	-2.5037, 59.7992	2013/12/17 4:00	-1.6710, 59.9279
	15	2013/12/17 4:00	-1.6606, 59.8649	2013/12/19 4:00	-1.5451, 60.0521

2.2 HF Radar Current

An HF radar system is a land-based technology capable of measuring surface currents for wide areas of the sea from backscattered radar signals reflected by ocean surface gravity waves (Barrick et al., 1977). The HF radar system works on the principle of Bragg scattering where the transmitted electromagnetic radio waves are reflected by resonant ocean surface waves with half of the incident radar wavelength. An HF radar system consists of a transmitter antenna transmitting high-frequency (3-50 MHz) electromagnetic waves over a conductive ocean surface and receiver antennas capturing the backscattered signal with a Doppler frequency shift resulting from the moving ocean surface due to waves and underlying (surface) currents.

Two Long Range SeaSonde HF radars by CODAR Ocean Sensors were installed in summer 2013 at North Ronaldsay and Sumburgh in northern Scotland, in the framework of the Brahan Project. This HF radar system delivered ocean current information in near real time, for an ocean surface area of two 180 km radius arcs either side of the Orkney-Shetland Channel (see Figures 1 and 4).Transmit frequencies were approximately 4.5 MHz. Current data obtained, representative of the first 2 meters of water column, have a spatial resolution of about 4.1 km and a temporal resolution of 1 hour. In Figure 4 a sample current map

obtained by the HF radar system is shown. Note that the HF radar system domain shown in Figure 4 defines the general domain for this work.

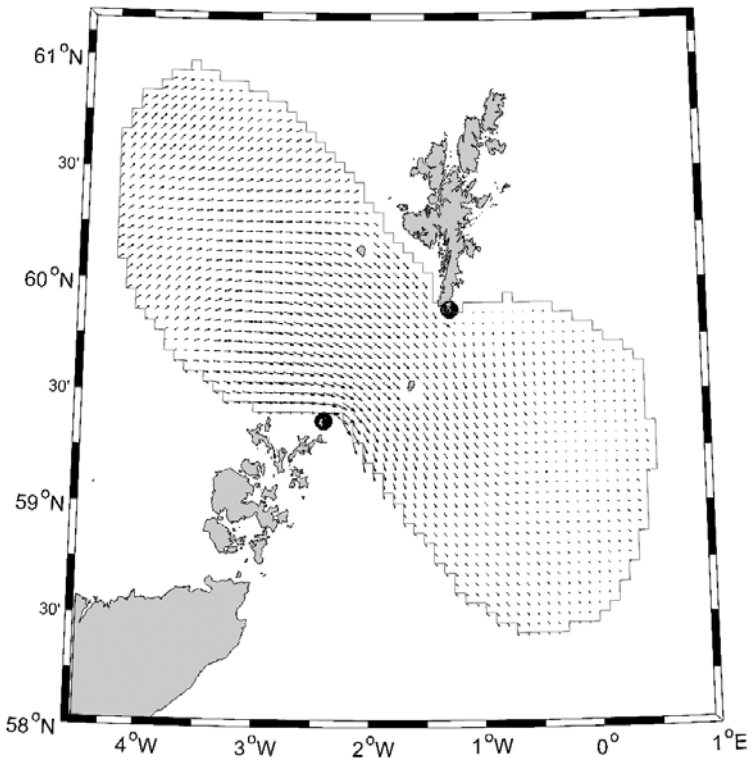

Figure 4 Example of the surface current map measured by the northern Scotland HF radar system. The radar site locations are indicated by solid black circles. The gray line defines the system domain limits.

2.3 Wind

For the calibration and validation of the oil spill transport model, wind data from the NOAA National Centers for Environmental Prediction (NCEP)'s Global Forecast System (GFS) Model (Environmental Modeling Center, 2003), with 0.5º spatial and 3-hourly temporal resolution, were used.

These data are served by the Center for Ocean-Land-Atmosphere Studies (COLA) using the GrADS - DODS/OPeNDAP Server (GDS) and by NOAA's National Operational Model Archive and Distribution System (NOMADS) Server.

2.4 Oil Spill Transport Model

The TESEO (Abascal et al., 2007) oil spill model was used in this study. The numerical model consists of a transport and a weathering module to represent the evolution of oil spilled in the marine environment. This work focuses on the use of the transport module, which is described below.

The transport application has been developed from the two-dimensional Lagrangian transport model PICHI, developed by the University of Cantabria as a part of the operational forecasting system created in response of the *Prestige* oil spill (Castanedo et al., 2006). The drift of the spilled oil is replicated by tracking a cloud of numerical particles representing the oil slicks. The position of the particles is computed by the superposition of the transport induced by currents, wind and turbulent dispersion. The numerical model solves the following vector equation:

$$\frac{d\vec{x}}{dt} = \vec{u}_a\left(\vec{x}_i, t\right) + \vec{u}_d\left(\vec{x}_i, t\right) \quad (1)$$

where $\vec{x}_i$ is the particle position and $\vec{u}_a$ and $\vec{u}_d$ are the advective and the diffusive velocities, respectively, in $\vec{x}_i$. The advective surface velocity $\vec{u}_a$ is calculated as the linear combination of currents and wind velocity expressed as

$$\vec{u}_a = C_C\,\vec{u}_c + C_D\,\vec{u}_w \quad (2)$$

where $\vec{u}_c$ is the surface current velocity, $\vec{u}_w$ is the wind velocity at a height of 10 m over the sea surface and C_D is the wind drag coefficient. Given the spatial scale of application of the model in this work, the Stoke's drift has been discarded with respect to the effect of winds and currents on the oil spill transport.

Note that Eq. (2) contains a coefficient in the current term, C_C. Usually, in Lagrangian models, the current term is not modified by any coefficient. However, when actual drift data are available and thus model coefficients can be calibrated, this parameter allows to take into account a possible under- or overestimating of the current fields, improving the accuracy of the performed simulations.

The turbulent diffusive velocity is obtained by Monte Carlo sampling in the range of velocities $\left[-\vec{u}_d, \vec{u}_d\right]$ that are assumed proportional to the diffusion coefficients (Maier-Reimer and Sündermann, 1982; Hunter et al., 1993). The velocity fluctuation for each time step, Δt, is defined as

$$\left|\vec{u}_d\right| = \sqrt{\frac{6D}{\Delta t}} \quad (3)$$

where D is the diffusion coefficient, typically in the range of 1-100 m^2/s (ASCE, 1996).

A total of 1000 independent numerical particles were used in every simulation, the diffusive coefficient was set to D = 50 m^2/s (ASCE, 1996) and a 60 s time step was used to calculate the time evolution of the particle positions.

2.5 Calibration

The objective of calibrating the oil spill transport model is to find the combination wind drag coefficient C_D and current coefficient C_C that minimizes the error between observed and simulated trajectories. The value of the wind coefficient C_D normally varies from 2.5 to 4.4 % of the wind speed, with a mean value of 3-3.5 % (ASCE, 1996). Although it is possible to use coefficients reported in the literature, work by Abascal et al. (2009a) showed the importance of obtaining the best-agreement coefficients for the region of interest.

As mentioned above, the pre-processing of the trajectory data collected during the drift experiments returned 27 trajectory sections of 48 h inside the HF radar domain with no gaps. The 12 sections obtained by pre-processing the drift data of the first exercise (see Table 1), and shown with different colors in Figure 5, were used in the calibration process.

The optimal coefficients of the model were obtained by the global optimization algorithm Shuffled Complex Evolution method (Duan et al., 1992) developed by the University of Arizona (SCE-UA). This method is an effective way to solve highly nonlinear

problems and is widely used in the automatic calibration of watershed models. The SCE-UA method is based on a synthesis of four concepts: (1) a combination of deterministic and probabilistic approaches; (2) a systematic evolution of a "complex" of points spanning the parameter space in the direction of global improvement; (3) competitive evolution; and (4) complex shuffling.

Following this methodology, the oil spill model calibration was formulated as an optimization problem where an objective function *J* has to be minimized. The objective function was defined as

$$J(\theta) = \frac{\sqrt{\sum_{i=1}^{N}\sum_{t=1}^{T}\left[\vec{x}_{i,t}^{O} - \vec{x}_{i,t}^{S}(\theta)\right]^2}}{N \cdot T}. \quad (4)$$

Eq. (4) represents the root-mean-square error (RMSE) between observed drifter positions $\vec{x}^O$ and the simulated ones $\vec{x}^S$. T is number of time steps of each buoy, N is the number of tracks used in the calibration process and $\theta = (C_C, C_D)$ is the vector of parameters to be optimized. In this case, T = 48 and N = 12.

Actual buoy positions $\vec{x}^O$ are the satellite-tracked drifter positions with a 1-h time step of the first deployment trajectory sections (see Table 2). Simulated buoy positions $\vec{x}^S$ are the centers of mass of the clouds of particles simulated by the transport model, forced with numerical wind and HF radar currents. Actual and simulated positions have the same time axis.

Thus the aim of the calibration was to find the optimal combination of the vector parameter $\hat{\theta} = (\hat{C}_C, \hat{C}_D)$ that minimizes the overall RMSE between actual and simulated trajectories.

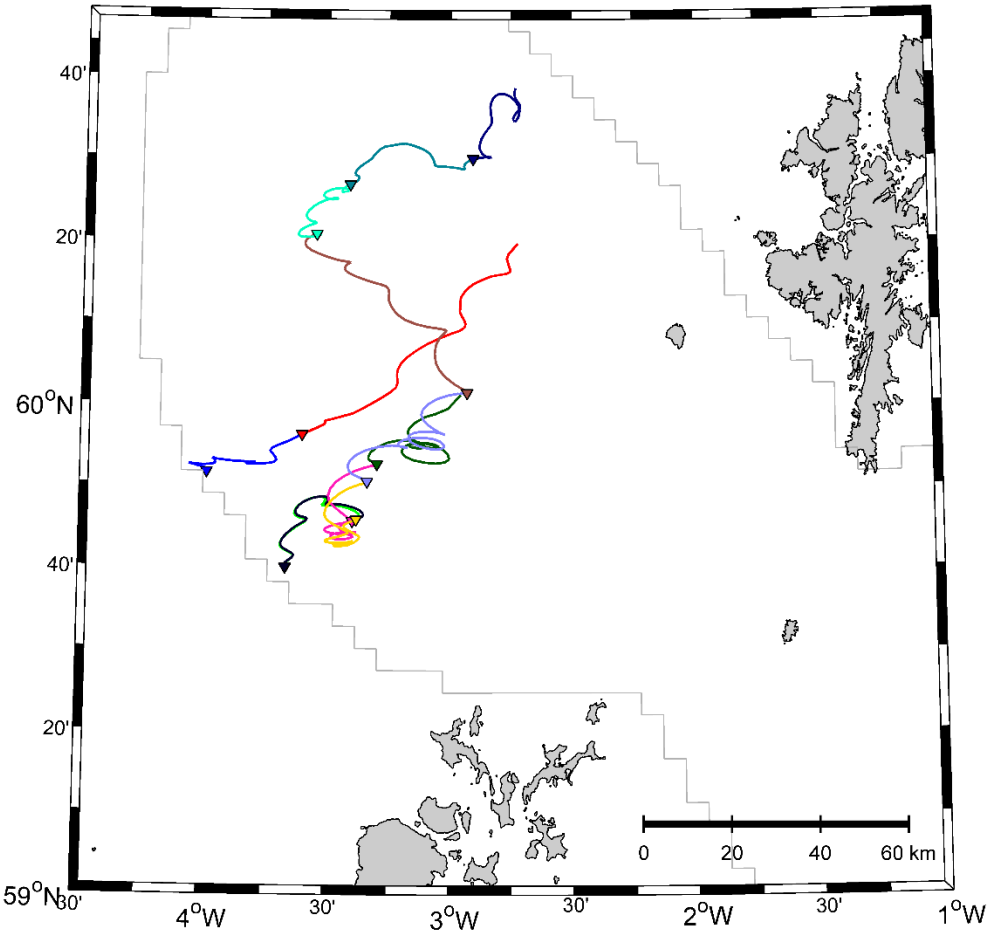

Figure 5 Track sections from the first drifter deployment, used in the calibration of the transport model. Triangles show the initial point of each section.

2.6 Validation

Once calibrated, the model was used to simulate the second dataset of trajectories shown in Table 1 and represented in Figure 6.

The quantification of the difference between the actual drifter paths and the model simulations was calculated by: (a) the time evolution of the distance error between the observed position and the position of the center of mass of the simulated particle cloud, (b) the RMSE between observed and simulated positions, for each track section during the second drifter deployment (Eq. 5), and (c) the overall RMSE between actual and simulated positions (calculated as the mean RMSE for all the track sections). The RMSE was defined as

$$RMSE = \frac{\sqrt{\sum_{i=1}^{T}\left(\vec{x}_i^{\,O} - \vec{x}_i^{\,S}\right)^2}}{T} \qquad (5)$$

where $\vec{x}^{\,O}$ is the observed drifter position at time step i, $\vec{x}^{\,S}$ is the position of the center of mass of the numerical particle cloud for the same time step and T is the number of time steps of the trajectory.

Moreover, the RMSE was expressed as a percentage of the distance travelled by the drifter for each track section.

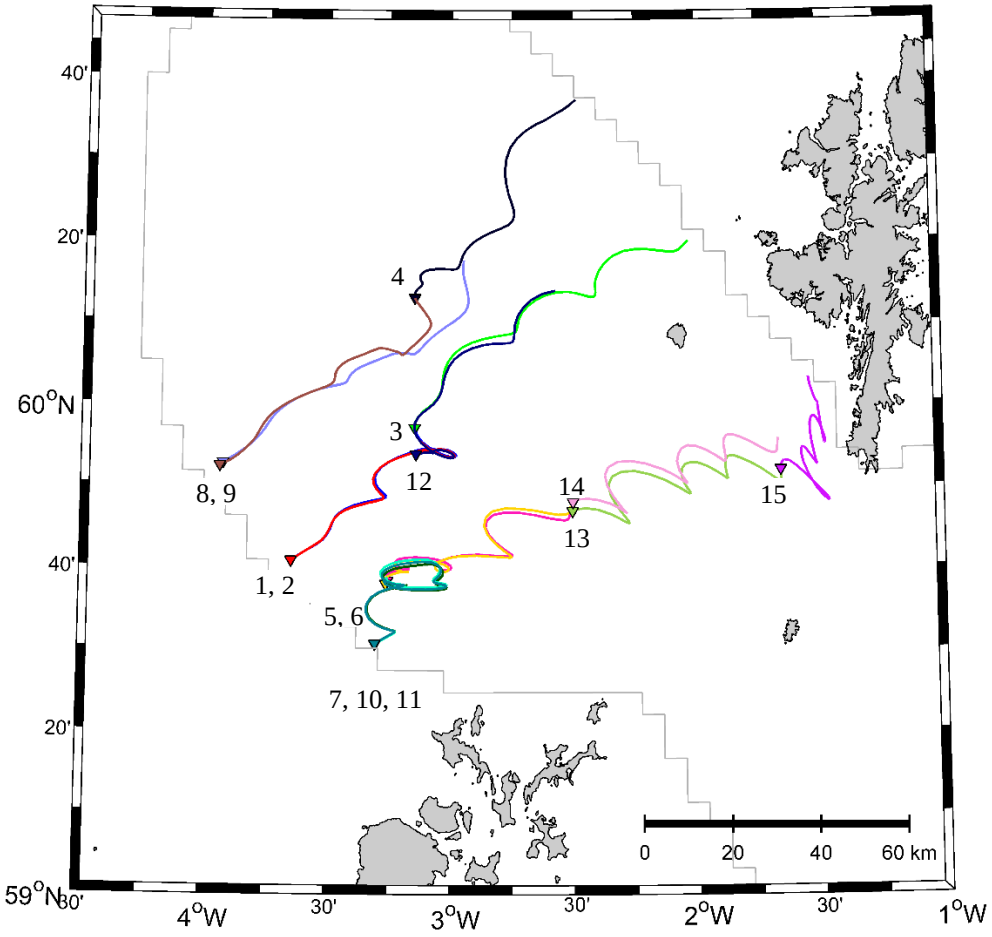

Figure 6 Track sections from the second drifter deployment, used in the validation of the transport model. Triangles show the initial point of each section. Numbers identify track sections as listed in Table 1.

3 Results

3.1 Calibration Results

By applying the SCE-UA method, the optimal combination of wind drag coefficient C_D and the current coefficient C_C that minimized Eq. (4) were $\hat{C}_D$ = 0.00015 and $\hat{C}_C$ = 1.14.

The C_C coefficient represents the effect of the current on the trajectories of the drifters, so a value close to 1, such as the one obtained in this study, demonstrates a good agreement between the drifter-derived current field and the radar HF current measurements. The C_D coefficient was found to be close to 0, suggesting that the contribution of atmospheric fields to simulate the drifter trajectories could be discarded. The value of the wind coefficient C_D normally varies from 2.5 to 4.4 % of the wind speed, with a mean value of 3-3.5 % (ASCE, 1996). The small value obtained for the wind drag coefficient C_D in this study is related to the low-profile drifter design, aimed at minimizing wind effect.

3.2 Validation Results

In order to validate the system, trajectory sections from the second exercise were simulated by the model with the optimal coefficient combination found in the calibration process: $\hat{C}_D$ = 0.00015 and $\hat{C}_C$ = 1.14. Note that, using these parameters, simulations are actually forced with negligible wind effect ($\hat{C}_D$ close to 0) and with nearly unchanged HF radar currents ($\hat{C}_C$ close to 1).

In Figures 7 and 8, the comparison for all the tracks is presented. Note that, for clarity, the numerical particle clouds are not shown but only the corresponding centers of mass and the 15 tracks are distributed across two Figures. Even though some differences exist, a good agreement with the model can be observed.

For conciseness, a more detailed comparison between observations and simulations is shown for three sections only: 4, 6 and 13. However, a quantification of the distance errors between actual and numerical trajectories will be presented for all the tracks later in the paper.

In Figures 9, 10 and 11 the comparison between actual and simulated trajectories for sections 4, 6 and 13 is presented. Note that the ocean area covered by the simulated particles represents the area where the drifting object most likely should be, according to the model. With that in mind, although some portions of the actual trajectories stay outside of the simulated areas, especially for track section number 6, the model shows a significant capability to capture most of the marked changes in the direction of drifter trajectories. Such skill of the transport model is a direct consequence of the accuracy of the forcing fields provided by the HF radar system.

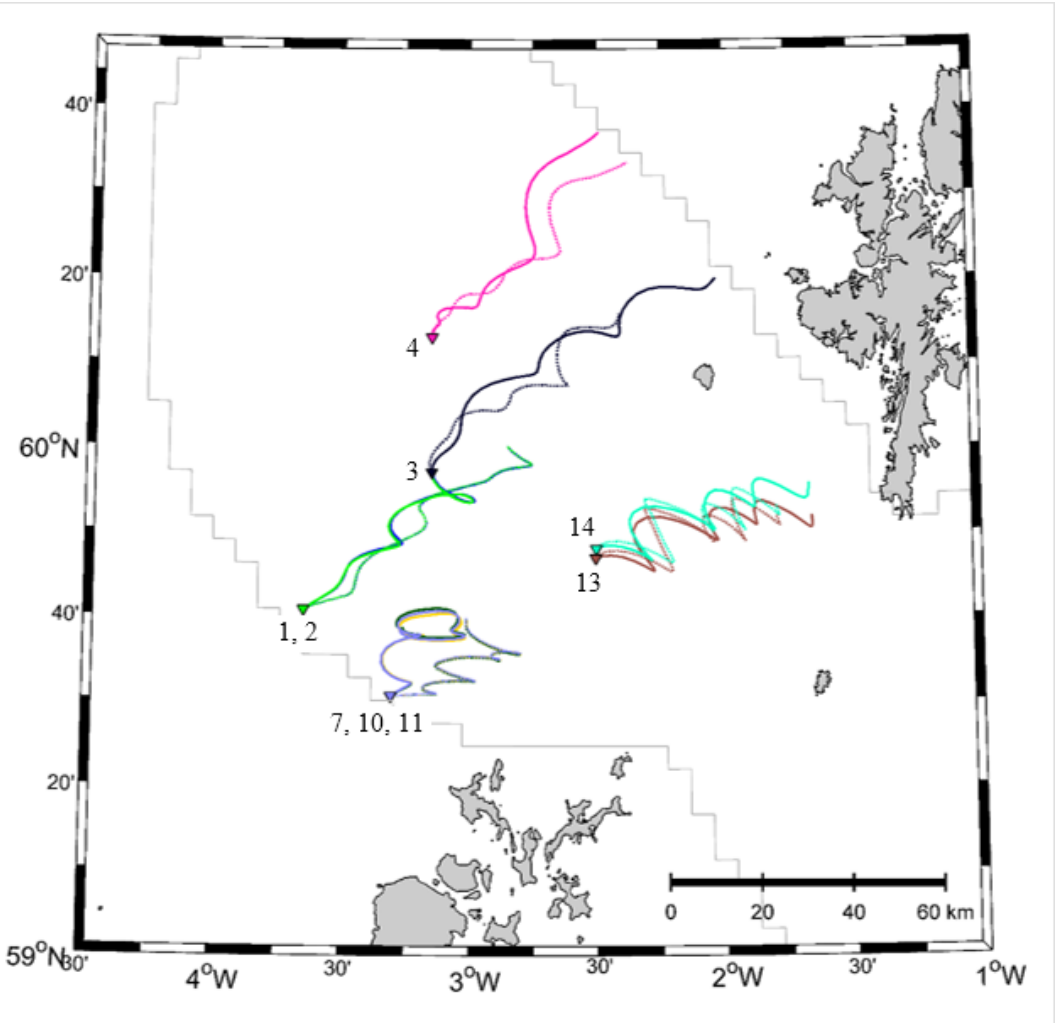

Figure 7 Comparison between actual (continuous lines) and simulated trajectories (dashed lines). Gray line represents the HF radar system domain limit. Numbers identify track sections as listed in Table 1.

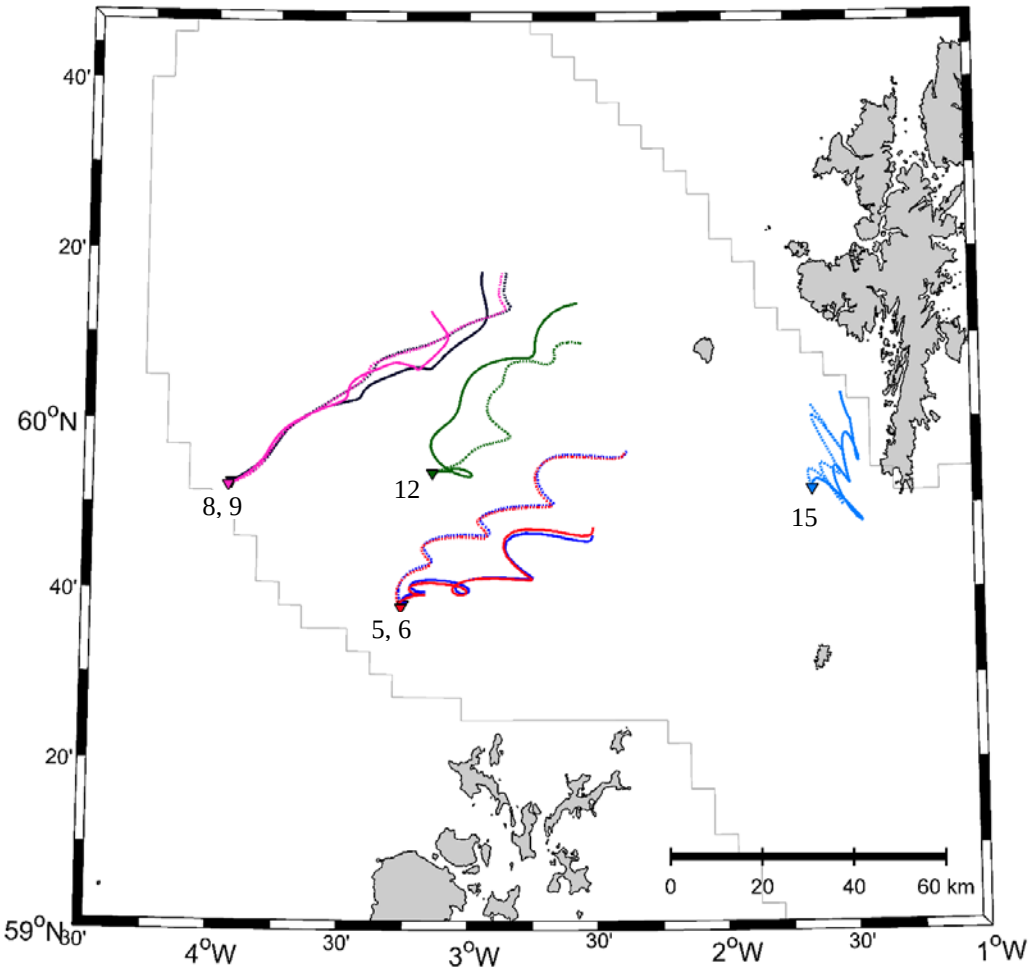

Figure 8 Comparison between actual (continuous lines) and simulated trajectories (dashed lines). Gray line represents the HF radar system domain limit. Numbers identify track sections as listed in Table 1.

The evolution of the distance error between observed locations and simulated cloud center of mass positions for these three tracks is presented in Figure 12. For track sections 4 and 13 (total length of 103 km and 141 km, respectively), the separation distance is less than 10 km over the 2-day simulation period. The error relative to track section 6 (144 km long) increases most during the first 24 hours, reaching 15 km, but subsequently remains fairly constant during the remainder of the simulation period. This result is in agreement with the trajectory comparison in Figure 10, which shows as, during the first part of the simulation, i.e. first couple of eddies, tracks diverge quite quickly at the beginning but subsequently maintain a reasonably parallel course.

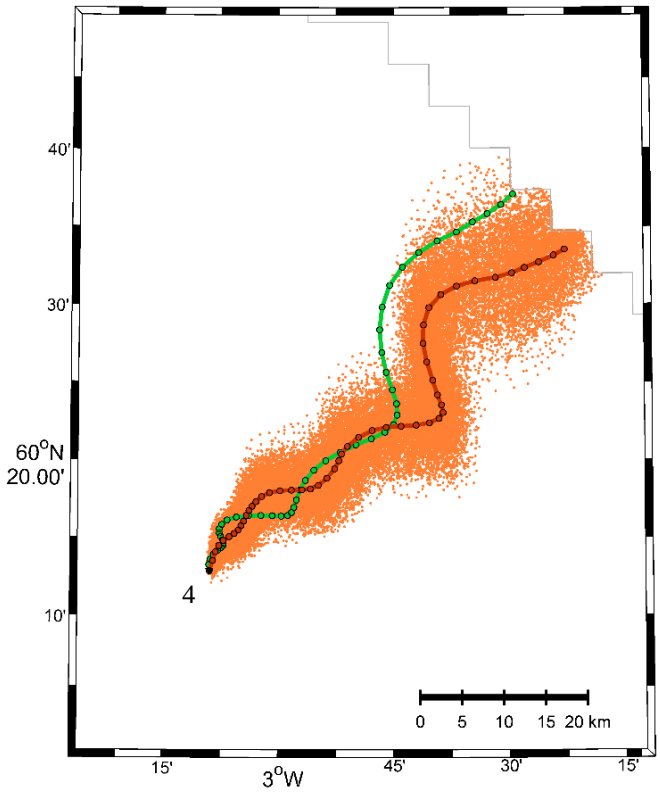

Figure 9 Comparison between observed positions (green filled circles joined by the green line) of track section 4 and the centre of mass of simulated particle positions (red filled circles joined by the red line). Simulated particle positions are shown as orange points.

Table 2 shows the RMSE obtained for each track during the second drifter deployment, the length of the tracks and the ratio between both values, which represent a measure of the error scaled to the length of the track. According to these results the lowest error obtained was 4.7 km for track 8 and the highest was 15.5 km for track 3, which is also one of the longest trajectories. When considering these errors relative to the distance covered by the drifters, they are always ≤10 % of the length of the tracks, with the maximum values found for tracks 3, 5, 7, 10 and 11, and the minimum of 4 % for tracks 8, 13 and 14. The overall RMSE was found to be 9.16 km for a mean track length of 123.2 km, corresponding to a mean deviation equal to 7 % of the distance covered by the buoy.

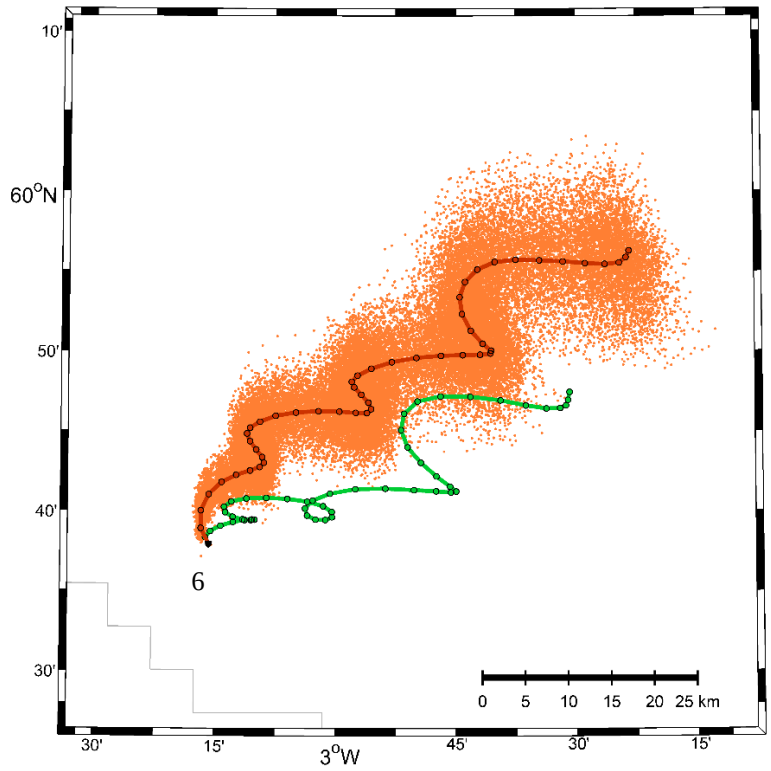

Figure 10 Comparison between observed positions (green filled circles joined by the green line) of track section 6 and the centre of mass of simulated particle positions (red filled circles joined by the red line). Simulated particle positions are shown as orange points.

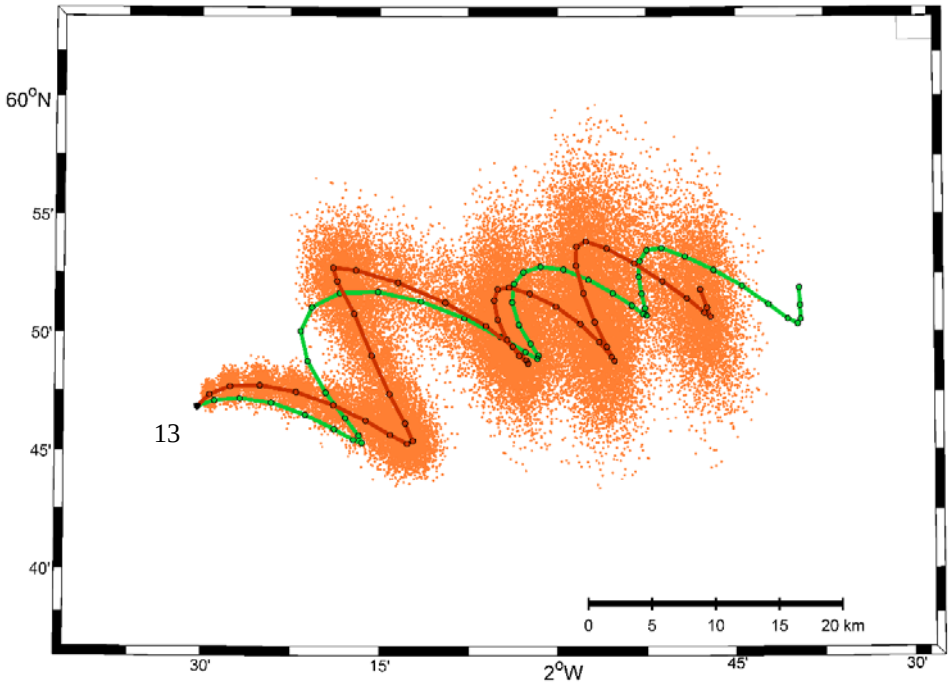

Figure 11 Comparison between observed positions (green filled circles joined by the green line) of track section 13 and the centre of mass of simulated particle positions (red filled circles joined by the red line). Simulated particle positions are shown as orange points.

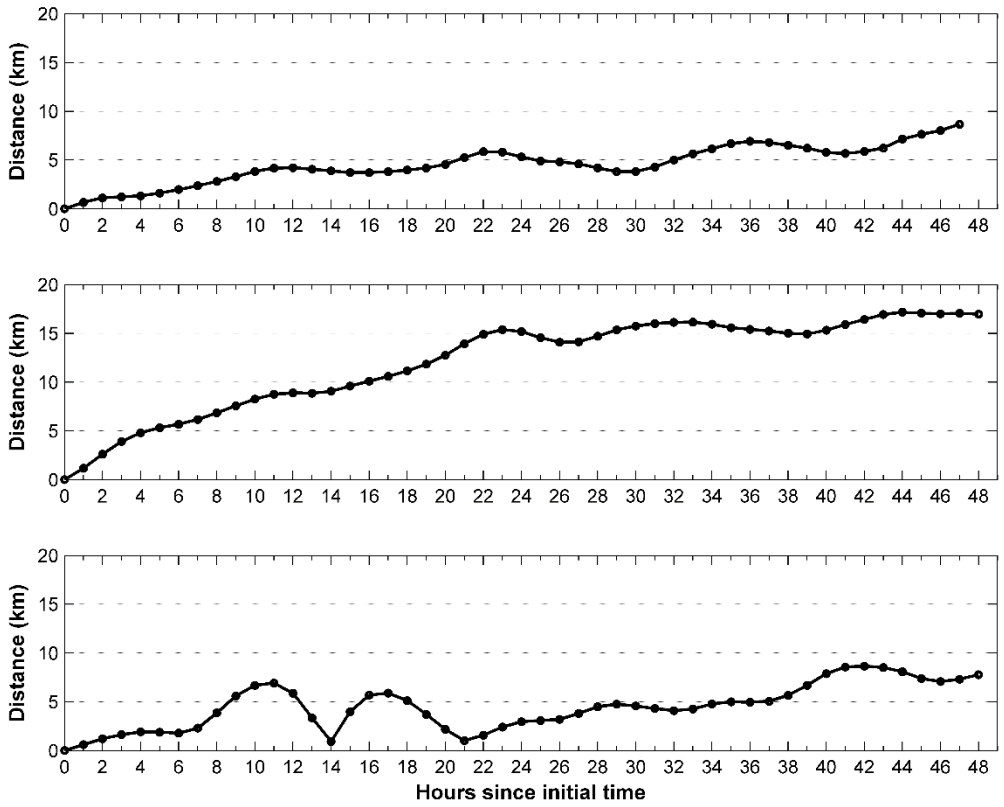

Figure 12 Evolution of the distance error between the actual and simulated drifter locations for track section 4 (upper panel), 6 (middle panel) and 13 (lower panel).

Table 2 Error analysis for track sections from the second drift exercise.

Section ID	RMSE (km)	Section length (km)	RMSE /Section length
1	8.6	113.8	0.08
2	8.8	112.1	0.08
3	14.5	142.2	0.10
4	4.9	103.1	0.05
5	13.6	139.5	0.10
6	13.0	144.2	0.09
7	11.8	122.9	0.10
8	4.7	128.8	0.04
9	7.8	113.3	0.07
10	12.3	120.5	0.10
11	12.1	120.8	0.10
12	9.4	115.6	0.08
13	5.0	140.5	0.04
14	5.4	141.4	0.04
15	5.5	90.0	0.06
Mean	9.16	123.2	0.07

4 Discussion

To have a reliable oil spill forecasting and backtracking system, a detailed calibration and validation of the oil transport model is required. Typically, oil spill models are calibrated using the drag coefficient values reported in the literature, or by means of a trial-and-error procedure using a single drifter buoy. The calibration methodology used in this study presents the following advantages: (1) no a-priori assumptions are made regarding the influence of the type of drifter (or the oil spill processes). This means that the dominant effect of currents or winds is not assumed but the actual technique estimates the relative importance of each forcing component; (2) the calibration methodology is based on a spatial approach integrating the information of a large dataset of drifters and therefore the obtained coefficients are representative of the study area; (3) the current coefficient included in the transport model allows to take into account a possible under- or overestimating of the current fields, improving the accuracy of the performed simulations.

As a result of the calibration, the optimal values of the parameters found were C_C = 1.14 and C_D = 0.00015. The high C_C value obtained (close to 1) indicates a good agreement between the drifter-derived current field and the radar HF current measurements. Note that the optimal C_C value is lightly greater than 1, which could be related to the drifter slippage (-2 cm/s slippage at a mean drift rate of 34 cm/s) in the along-drift direction mentioned in section 2.1. Lagrangian trajectory models. Abascal et al. (2009), using currents from global circulation models, estimated a value of C_C = 0.266, suggesting discrepancies between the real and numerical current fields. Sotillo et al. (2008), using currents from higher resolution nested regional circulation models, obtained C_C =0.52. These results showed that the C_C value was improved using current data provided by regional circulation models. However, discrepancies between the real and numerical current fields were still present. The high C_C value obtained in the present study (close to 1) shows the improvement of using observed HF radar currents regarding these previous works based on global and regional numerical models.

The wind drag coefficient is the most important coefficient in oil spill transport models. The value of the wind coefficient C_D normally varies between 2.5 and 4.4 % of the wind speed, with a mean value of 3-3.5 % (ASCE, 1996). In this study, C_D was found to be close to 0, suggesting that the contribution of atmospheric fields to simulated drifter trajectories could be discarded. Note that a reduction of the wind drag coefficient is expected when using HF radar currents, due to the capability of HF radar measurements to partially include the wind-driven component of the water velocity. However, the small value obtained in this study (close to 0) could also be related to the low-profile drifter design, aimed at minimizing wind effect or to the coarse spatial resolution of the wind data. These results suggest that the value of C_D obtained is the optimal to simulate this type of drifter buoy with this wind dataset, but is not the optimal to simulate oil spills. Based on previous studies (Abascal et al., 2009b; Abascal et al., 2012), a value of C_D = 0.02 is proposed for the oil spill forecasting and backtracking system.

Besides the influence of the type of drifter on the drifting trajectory, these results show the importance of properly determining the relative contribution of each forcing component in the transport and using the appropriate coefficients in order to optimize the model results.

Once calibrated, the model results were validated by comparison between actual and drifter trajectories. The model shows a significant capability to reproduce the drifter trajectories, which is a direct consequence of the accuracy of the forcing fields provided by the HF radar system. The accuracy of the simulations performed was measured by the RMSE between the actual locations of the drifter and the corresponding positions of the center of mass of the simulated particle clouds. After 48 hours of simulation the overall RMSE was found to be 9.16 km for a mean trajectory length of 132.2 km, which equates to an average

distance error between actual and simulated positions of approximately 7 % of the mean observed track length. These results show a good agreement between actual and simulated trajectories if compared with previous works of validation with drifting buoys (Price et al., 2006; Barron et al., 2007; Caballero et al., 2008; Sotillo et al., 2008; Abascal et al., 2009; Huntley et al., 2011; Cucco et al., 2012, De Dominicis et al., 2013) and the capabilities of HF radar currents for oil spill trajectory modelling.

5 Conclusions

In this paper an oil spill forecasting and backtracking system in the North Sea area based on HF radar currents is presented. The system is calibrated and validated by means of drifter trajectories collected during two drift experiments carried out in the Shetland-Orkney area. Data from the first deployment were used for calibration and data from the second for validation of the model.

As a result of the calibration, the optimal values of the parameters found were C_C = 1.14 and C_D = 0.00015. The high C_C value obtained (close to 1) indicates a good agreement between the drifter-derived current field and the radar HF current measurements and represents an improvement in relation to similar works performed with numerical currents forcing (Sotillo et al. (2008), Abascal et al. (2009)). Regarding C_D, the small value obtained (close to 0) could be related to the low-profile drifter design, aimed at minimizing wind effect.

The validation of the model shows its capability to properly reproduce the drifter trajectories, which is related to the accuracy of the forcing fields provided by the HF radar system. The average RMSE was found to be 9.16 km for a mean track length of 123.2 km (in 48 h), which shows a good agreement between actual and simulated trajectories.

This work highlights the benefits of using ocean current data measured by HF radar systems for trajectory simulation of drifting objects and oil spills. Moreover, this work also highlights that drifter exercises are of paramount importance to have reliable oil spill forecast systems, based on calibrated and validated oil spill transport models. However, for operational oil spill response applications, further work is required using trajectory data estimated from drifting devices. Moreover, further studies are required to analyze the differences between drifting buoys and oil slicks in order to select the appropriate type of drifting buoy to calibrate and validate oil spill transport models.

6 Acknowledgements

This work was partially funded (20%) from a grant from Iceland, Liechtenstein and Norway through the EEA Grants. MC would like to thank the Spanish Ministry of Economy and Competitiveness **(**MINECO) for the funding under the FPI Program.

7 References

Abascal, A.J., S. Castanedo, A.D. Gutierrez, E. Comerma, R. Medina and I.J. Losada, “TESEO, an Operational System for Simulating Oil Spill Trajectories and Fate Processes”, in *Proceedings of Seventeenth International Offshore Ocean and Polar Engineering Conference*, The International Society of Offshore Ocean and Polar Engineering, Lisbon, ISOPE, 3:1751-1758, 2007.

Abascal, A.J., S. Castanedo, R. Medina, I.J. Losada, E and Alvarez-Fanjul. “Application of HF Radar Currents to Oil Spill Modelling”, *Marine Pollution Bulletin*, 58:238-248, 2009b.

Abascal, A.J., S. Castanedo, V. Fernández and R. Medina, "Backtracking Drifting Objects using Surface Currents from High-frequency (HF) Radar Technology", *Ocean Dynamics*, 62:1073-1089, 2012.

ASCE Task Committee, "State-of-the-art Review of Modeling Transport and Fate of Oil Spills", *Journal of Hydraulic Engineering*, 122(11):594-609, 1996.

Barrick, D., M.W. Evens and B.L. Weber, "Ocean Surface Currents Mapped by Radar", *Science*, 198:138-144, 1977.

Barron, C.N., L.F. Smedstad, J.M. Dastugue and O.M. Smedstad, "Evaluation of Ocean Models Using Observed and Simulated Drifter Trajectories: Impact of the Sea Surface Height on Synthetic Profiles for Data Assimilation", *Journal of Geophysics Research*, 112(C7), 2007.

Berx, B., J. Dunn, M. Geldart, S. Hughes and D. Lee. "MSS Davis CODE Drifter". Marine Scotland Science Report. 2014. Retrieved March, 2015 from: http://www.gov.scot/Resource/0046/00461208.pdf

Caballero, A., M. Espino, Y. Sagarminaga, L. Ferrer, A. Uriarte and M. González, "Simulating the Migration of Drifters Deployed in the Bay of Biscay, during the *Prestige* Crisis", *Marine Pollution Bulletin*, 56:475-482, 2008.

Castanedo, S., R. Medina, I.J: Losada, C. Vidal, F.J. Méndez, A. Osorio, J.A. Juanes and A. Puente, "The *Prestige* Oil Spill in Cantabria (Bay of Biscay) Part I: Operational Forecasting System for Quick Response, Risk Assesment and Protection of Natural Resources", *Journal of Coastal Research*, 22(6):1474-1489, 2006.

Chapman, R.D., L.K. Shay, H.C. Graber, J.B. Edson, A. Karachintsev, C.L. Trump and D.B. Ross, "On the Accuracy of HF Radar Surface Current Measurements: Intercomparisons with Ship-based Sensors", *Journal of Geophysics Research*, 102(8):18737-18748, 1997.

Chapman, R.D. and H.C. Graber, "Validation of HF radar measurements", *Oceanography*, 10:76-79, 1997.

Cucco, A., M. Sinerchia, A. Ribotti, A. Olita, L. Fazioli, A. Perilli, B. Sorgente, M. Borghini, K. Schroeder and R. Sorgente, "A High-resolution Real-time Forecasing System for Predicting the Fate of Oil Spills in the Strait of Bonifacio (Western Mediterranean Sea)", *Marine Pollution Bulletin*, 64:1186-1200, 2012.

Davis, R.E., "Drifter Observations of Coastal Surface Currents during CODE: the Method and Descriptive View", *Journal of Geophysical Research*, 90(C3):4741-4755, 1985.

De Dominicis, M, N. Pinardi, G. Zodiatis and R. Archetti, "MEDSLIK-II, a Lagrangian Marine Surface Oil Spill Model for Short-term Forecasting – Part 2: Numerical Simulations and Validations", *Geoscientific Model Development*, 6:1871-1888, 2013.

Duan, Q., S. Sorooshian and V. Gupta, "Effective and Efficient Global Optimization for Conceptual Rainfall-runoff Models", *Water Resources Research*, 28(4):1015-1031, 1992.

Edwards, K.P., F.E. Werner and B.O. Blanton, “Comparison of Observed and Modeled Drifter Trajectories in Coastal Regions: an Improvement through Adjustments for Observed Drifter Slip and Errors in Wind Fields”, *Journal of Atmospheric and Oceanic Technology*, 23(11):1614-1620, 2006.

Environmental Modeling Center, (2003). *The GFS atmospheric Model*. NOAA/NCEP/Environmental Modeling Center Office Note 442, 14pp. Retrieved March, 2015 from http://www.emc.ncep.noaa.gov/officenotes/FullTOC.html

González, M., A. Uriarte, R. Pozo and M. Collins, “The Prestige Crisis: Operational Oceanography Applied to Oil Recovery, by the Basque Fishing Fleet”, *Marine Pollution Bulletin*, 53:369-374, 2006.

Huntley, H.S., B.L.J. Lipphardt and A.D.J. Kirwan, “Lagrangian Predictability Assessed in the East China Sea”, *Ocean Modelling*, 36:163-178, 2011.

Hunter, J.R., P.D. Craig and H.E. Phillips, “On the Use of Random Walk Models with Spatially Variable Diffusivity”, *Journal Comparative Physiology*, 106:366-376, 1993.

Kohut, J.T., H.J. Roarty, and S.M. Glenn, “Characterizing Observed Environmental Variability with HF Doppler Radar Surface Current Mappers and Acoustic Doppler Current Profilers: Environmental Variability in the Coastal Ocean”, *Journal of Oceanic Engineering*, 31(4):876-884, 2006.

ITOPF, (2014), The International Tanker Owners Pollution Federation Ltd, *Oil Tanker Spill Statistics*. Retrieved March, 2015 from: www.itopf.com/

Maier-Reimer, E. and E. Sündermann, “On Tracer Methods in Computational Hydrodynamics”, in *Engineering Application of Computational Hydraulics, 1*, Chap 9, M.B. Abbott and J.A. Cunge (eds.), Pitman, London, pp. 198-217, 1982.

Montero, P., J. Blanco, J.M. Cabanas, J. Maneiro, Y. Pazos, A. Moroño, C.F. Balseiro, P. Carracedo, B. Gomez, E. Penabad, V. Pérez-Muñuzuri, F. Braunschweig, R. Fernandes, P.C. Leitao and R. Neves, “Oil Spill Monitoring and Forecasting on the *Prestige-Nassau* Accident”, *Proceedings of the Twenty-sixth AMOP Technical Seminar*. Environment Canada, Ottawa, ON, pp. 1013-1029, 2003.

Price, J.M., M. Reed, M.K. Howard, W.R. Johnson, Z. Ji, C.F. Marshall, N.L. Guinasso and G.B. Rainey, “Preliminary Assessment of an Oil-spill Trajectory Model using a Satellite-tracked, Oil-spill-simulating Drifter”, *Environmental Modelling and Software*, 21:258-270, 2006.

Sotillo, M.G., E. Alvarez Fanjul, S. Castanedo., A.J. Abascal, J. Menendez, R. Olivella, E. García-Ladona, M. Ruiz-Villareal, J. Conde, M. Gómez, P. Conde, A.D. Gutierrez and R. Medina, “Towards an Operational System for Oil Spill Forecast in the Spanish Waters: Initial Developments and Implementation Test”, *Marine Pollution Bulletin*, 56(4):686-703, 2008.